Behavior of Ethylene glycol Addition on the Physico-Chemical and Mechanical Properties of Alkali Activated Slag and its Resistivity to Sulfate

Ahmed A. Amer*, Mohamed Arif
Chemistry Department, Faculty of Science, Zagazig University, Zagazig, Egypt

Abstract— This paper reports the results of investigation on the influence of ethylene glycol (EG) addition on the physico-chemical and mechanical properties of alkali-activated slag (AAS) pastes as well as its resistivity to 5 % $MgSO_4$ solution. Granulated blast furnace slag (GBFS) was activated by 6 wt., % NaOH (SH) or mixture of liquid sodium silicate (LSS) and SH (3% SH : 3 % LSS) with/without 5 wt., % EG. The results show that, the setting times of M0-SH/LSS paste elongate with the addition of EG, A significant increase of the chemically combined water content of AAS paste with EG. The addition of EG to activated GBFS-SH system has a positive effect on the compressive strength, while its addition to GBFS-SH/LSS has a negative effect. EG reduces the drying shrinkage by ≈ 34 and 32 % for GBFS activated by SH or SH/LSS, respectively. It can be concluded that AAS is more durable in $MgSO_4$ solution than SRC paste. Moreover, some selected samples were investigated by using TG, DTG, FTIR and SEM techniques analyses.

Index Terms—AAS, EG, Compressive strength, drying shrinkage, GBFS, TG/DTG

1 INTRODUCTION

The production of Portland cement (OPC) consumes sizable energy and emits a large volume of greenhouse gas to the atmosphere. Therefore, alkali activated materials have attracted great attention in recent years because of its numerous advantages such as excellent mechanical properties [1-3], high resistance to chemical attack and durability [4-6], thermal stability [7,8] and low pollutant greenhouse gas emission [9]. Industrial by-product such as Granulated Blast Furnace Slag (GBFS) has an important place today's concrete technology owing to their positive effects on the durability, strength of concrete and low production costs. GBFS is the most common mineral admixtures utilized as an ingredient in cement or concrete manufacturing [10]. It is a glassy granular material formed by rapidly cooled of molten GBFS and then ground to improve its reactivity. Its hydraulic reactivity depends on its chemical composition, glass phase content, particle size distribution and surface morphology [11].

Alkali-activated slag (AAS) is produced by activating GBFS with an alkaline activator. The commonly used alkali activators in AAS are sulfate, OPC, Na_2SiO_3 and NaOH. AAS can be used to manufacture cementitatious pastes and concretes without the need of traditional OPC. GBFS represented precursor of calcium enriched system and the reaction product is a C-S-H (I) gel, similar to that found in OPC with a lower Ca/Si ratio and a high Al incorporation [12,13]. Caustic alkalis or alkali compounds whose anions can react with Ca^{2+} to form compounds less soluble than $Ca(OH)_2$ which can act as activators for slag. The use of sodium silicate based activator ($Na_2SiO_3.H_2O$ + NaOH) has been found to be ideal to produce desired mechanical properties [14-16].

In the last years, geopolymer composites have been introduced. Geopolymer composites are usually obtained by incorporation of organic polymers [17-22] such as polyvinyl acetate, polyvinyl alcohol, polypropylene and water soluble organic polymers [23-27]. Recently, Ferone et al., [28] have prepared novel organic-inorganic hybrid composites, adding epoxy resins to geopolymer, through an innovative synthetic approach based on a co-reticulation in mild conditions of organic and inorganic components, producing an intimate as well as inorganic one. In a previous work [29], the effect of ethylene glycol [EG] admixed on the physico-chemical and mechanical properties of GBFS activated by 6 wt, % NaOH solution was studied. The results show that, the setting times of pastes elongated with EG, the drying shrinkage was reduced by ≈ 7, 28, 53 and 68 % in case of AAS containing 2.5, 5, 7.5 and 10 wt% EG up to 7 days, respectively. The wet compressive strength decreased with EG. Whereas, the dry compressive strength of AAS dried at 80 °C for 24 h increased with EG up to 7.5 wt,%. El-Didamony et al [4] studied the properties and durability of AAS pastes immersed in sea water. It can be concluded that AAS showed good durability in sea water up to 12 months comparing with SRC paste in the same conditions. Komljenović et al., [30] studied the effect of external sulfate attack on mechanical properties of alkali activated slag and CEMII (OPC blended with slag). AAS showed significantly higher resistance to sulfate attack with respect to benchmark CEM II. Bakharev et al., [31] found that AAC concrete of Grade 40 has a high resistance in acetic acid environment. The aim of the present work is to study the hydration kinetics of AAS activated by sodium hydroxide SH or sodium silicate based solution (LSS + SH) with/without 5 wt,% EG.

• Corresponding author
Ahmed A. Amer (Ph.D)
E.mail: drahmed.amer@zu.edu.eg
Tel. +201210088668

2. MATERIALS AND METHODS OF INVESTIGATION

2.1. Materials

The materials used in this research are GBFS, provided by Iron and Steel Company, Helwan Governorate, Egypt. Sulfate resisting cement (SRC) is obtained from Suez Cement Company, Suez plant, Suez, Egypt. Sodium hydroxide (SH) was brought from SHIDO Company with purity 99%, liquid sodium silicate (LSS) consists of 32% SiO_2& 17% Na_2O with silic modulus SiO_2/Na_2O equal 1.88 and density 1.46 g/cm^3, and EG with assay 99% and density 1.11 g/cm^3 were purchased from El-Goumhourya Chemical Company, Egypt. The chemical composition of GBFS and SRC are seen in Table (1). Fig. (1) shows the XRD pattern of GBFS, which confirms the amorphous character. From the chemical composition, it is clear that GBFS is mainly composed of CaO: 38.70, MgO: 7.11 and Na_2O: 1.03 wt% as basic oxide and acidic oxide of SiO_2: 37.81 wt%. The basicity coefficient of GBFS (K_b) is: (CaO + MgO) / SiO_2 equal to 1.2, therefore, it has a basic character. GBFS particle morphologies were examined using Scanning Electron Microscopy (SEM) is presented in Fig. (2). It is mainly composed of pyramid like particles with an average size of 7 μm. The micrograph also shows some irregular shape particles with a dense-compact structure with an average size of 20 μm.The particle size distribution of GBFS has about 90% < 50 and 10% < 7 μm.

Table 1: Chemical composition of raw materials, wt,%

Oxide content (%)	*GBFS*	*SRC*
SiO_2	37.81	21.90
Al_2O_3	13.14	4.15
Fe_2O_3	0.23	5.18
CaO	38.70	62.91
MgO	7.11	2.16
Na_2O	1.03	0.48
K_2O	0.19	0.11
SO_3	1.19	1.8
P_2O_5	0.17	0.00
L.O.I.	0.03	0.58
TOTAL	99.60	99.27

Table 2: Mix composition of GBFS activated pastes

MIX	GBFS,%	SH, %	LSS, %	EG, %
M0-SH	100	6	0	0
M0-SH/LSS	100	3	3	0
M5-SH	100	6	0	5
M5-SH/LSS	100	3	3	5

The GBFS was firstly ground to pass through a 2 mm diameter sieve. The material was completely passed through a magnet to remove any contamination of iron melt in the GBFS, then ground in a steel ball mill to pass through 45 μm sieve. The surface area of GBFS was 4500±50 cm^2/g. Different mixes were prepared as shown in Table (2). The pastes were prepared using SH and LSS activator at 6 wt% of dry mixes at water/slag (W/S) ratio of 0.25. EG was added to GBFS activated with SH or SH/LSS from 0 to 5 wt%. GBFS was mixed with alkali activator in the mixing water with/without EG for 5 minutes using a mixer (HOBART, model N50, Canada). The mixer was stopped to collect any unmixed solids scraped from the sides of the mixing bowl and the paddle into the bowl. 2 more minutes of slow mixing and 5 minutes of fast mixing were applied to ensure homogeneity. For each mix, the freshly prepared cement paste was placed into one inch cubic moulds and strong manually pressed into the corner and along the surface of the mould, then vibrated using vibration machine for one min. After compaction of the top layer, the surface of the paste was smoothed by thin edged trowel. The mould cured in humidity chamber (100% RH) at room temperature for 24 h, then demoulded and cured under tap water up to 3, 7, 28 and 90 days. For the pastes, which were tested for resistivity against $MgSO_4$ attack, were cured up to 28 days (zero time) under tap water and then immersed in 5 % $MgSO_4$ solution for one, 3, 6 and 9 months. The hydration of the pastes was stopped using an acetone-methanol mixture [4], then dried at 70 °C for 2 hours, and kept in airtight containers.

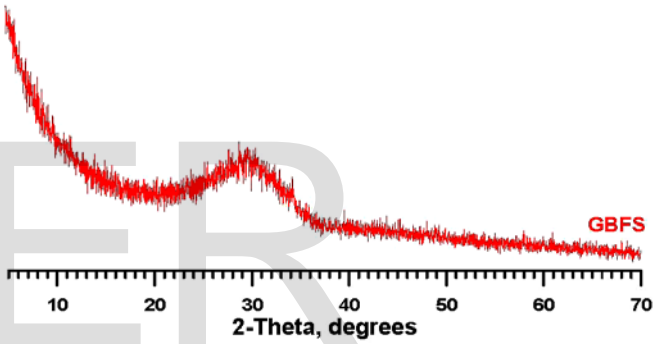

Fig. 1 XRD pattern of GBFS

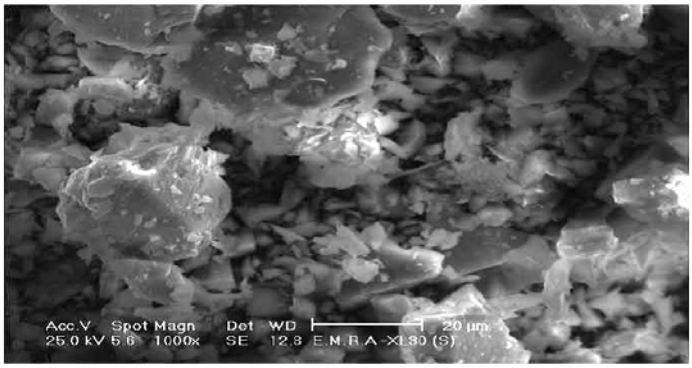

Fig. 2 SEM photograph of GBFS

2.2. Methods of investigation

The initial and final setting times were both measured using the Vicat Apparatus according to ASTM C191 [32]. The combined water contents (Wn, wt%) were determined from the ignition loss of the dried paste on the ignition weight basis at 900 °C for 20 min. [33]. The combined water content was

calculated as: Wn = [(W1 – W2) / W2] – (L)], where, Wn: is the combined water, W1: is the weight of dried paste before ignition, W2: is the ignition weight of specimen, and L: is the ignition loss of unhydrated specimen. The compressive strength of the pastes was measured according to ASTM C109M [34]. Shrinkage was also determined according to ASTM C490 [35]. The length change of activated slag mortar with/without magnesium oxide at any age was calculated as: A = (Ax – Ai) / G; where, A: change in length at x age %, Ax: comparator reading of specimen at x age minus comparator reading of reference bar at x age, Ai: initial comparator reading of specimen minus comparator reading of reference bar at the same time and G: is the nominal gauge length, 285 mm. Thermo-gravimetric analysis (TGA) were carried out by heating the sample in nitrogen atmosphere up to 1000 °C with a heating rate of 20 °C/min using a DT-50 Thermal Analyzer (Schimadzu Co-Kyoto, Japan). Infrared spectral analysis was carried out on some selected samples of hydrated paste to provide additional information on the hydrated products. The infrared spectral analysis was recorded from KBr discussing Genesis FTIR spectrometer in the range of 400-4000 cm^{-1}. The scanning electron micrographs were taken with Inspect S (FEI Company, Holland) equipped with an energy dispersive X-ray analyzer (EDX) to examine the microstructure of the fractured composites at the accelerating voltage of 200 V to 30 kV and power zoom magnification up to 300000 xs.

3. RESULTS AND DISCUSSION

3.1. Setting times

The initial and final setting times (IS and FS) of GBFS activated by SH or SH/LSS containing 0 or 5 wt% EG (M0-SH, M0-SH/LSS, M5-SH and M5-SH/LSS) are graphically represented in Fig. (3). It is clear that, the initial and final setting times of M0-SH/LSS are longer than M0-SH. This is due to LSS increase the viscosity of the medium leading to the formation of hydration products with more gel character than those formed in absence of LSS (M0-SH). Also, the addition of EG to each activated paste elongates the setting times, this is attributed to its high significant effect on M5-SH/LSS activated paste. EG acts as a dehydrating agent for sodium silicate forming a high amount of silica gel which in turn significantly elongates the initial and final setting times [36].

3.2. Chemically combined water, (Wn, wt%)

The chemically combined water of GBFS activated by SH or SH/LSS with/without 5 wt% EG cured in tap water (TW) at room temperature are graphically plotted in Fig. (4). Generally, the Wn, % content of M0-SH and M0-SH/LSS gradually increases with curing time, demonstrated that the amount of hydration products increase with time. The Wn, % M0-SH/LSS or M5-SH/LSS is lower than that of M0-SH paste at all ages of hydration. This finding related to that, the amount of silicate species increases with the addition of LSS; these silicates are responsible for the consumption of the remained CH in the system forming additional CSH in activated slag matrix. Meanwhile, the remained CH in M0-SH paste is carbonated by atmospheric CO_2 to form $CaCO_3$, which has a great effect on the values of Wn, %. In addition, the extent of polymerization increases with the silicate species which act as inorganic monomer forming hydration products with low content of Wn, % (the higher the degree of polymerization, the lower content of combined water). In M5-Sh and M5-SH/LSS pastes, the Wn, % decreases with curing time up to 28 days. This decrease may be caused by the polymerization of EG. At 90 days, Wn, % increases again in each two mixes, suggesting the increase of hydration products.

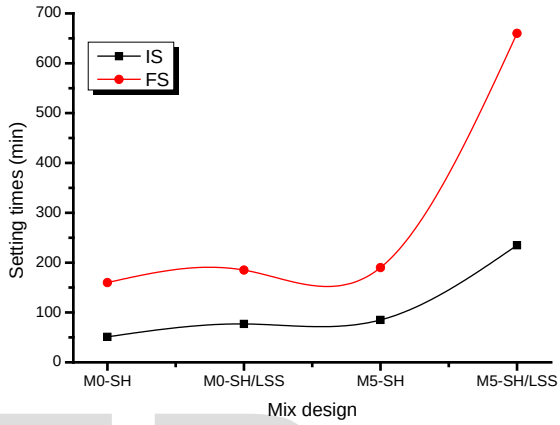

Fig. 3 Setting times of AAS pastes with/without EG

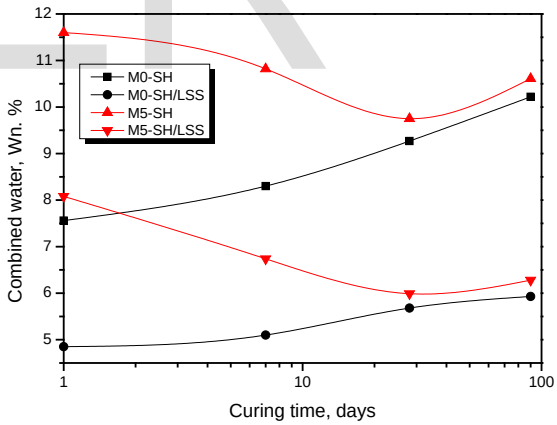

Fig. 4 Chemically combined water contents of different AAS with/without EG

3.3. Wet compressive strength

The wet compressive strength values of all hardened pastes M0-SH, M0SH/LSS, M5-SH and M5-SH/LSS cured in TW up to 90 days are graphically represented in Fig. (5). It is clear that, the compressive strength of hydrated paste M0-SH/LSS is higher than that activated by SH only (M0-SH) at all ages of curing. This fact may be attributed to that, LSS contains an amount of siloxnate groups $[SiO_4]^-$ which act as inorganic monomers reacting with retained CH in the system forming CSH as well as increase the polymerization of the hydrated

products. At one day of curing, the addition of 5 wt, % EG to GBFS activated by SH or SH/LSS reduces the compressive strength by ≈ 36 and 71 % respectively. This may be due to the viscosity of the medium increases with the addition of EG to GBFS-SH/LSS paste causing retardation of GBFS activation. Meanwhile, EG has a little effect on the retardation of GBFS-SH paste. At 90 days of curing, a significant increase in the compressive strength was observed with the addition of 5 wt, % EG to GBFS-SH compared with GBFS without EG. The addition of 5 wt,% EG to GBFS-SH paste increases the compressive strength value by ≈ 7.4; while the addition of EG to GBFS-SH/LSS decreases the compressive strength value by ≈ 23% compared with the reference at 90 days. This proves that the addition of EG to GBFS-SH system has a positive effect on the compressive strength while the addition of EG to GBFS-SH/LSS has a negative effect.

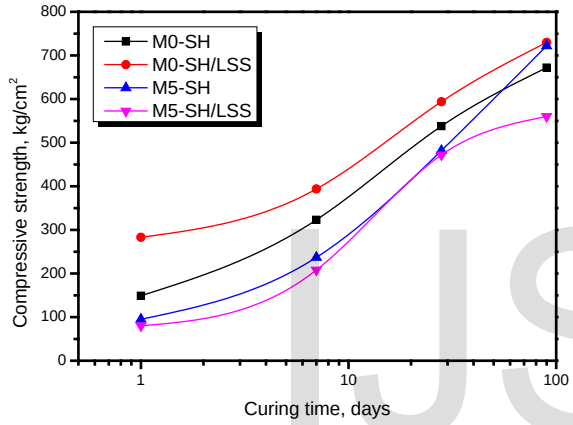

Fig. 5 Compressive strength of AAS pastes with/without EG

3.4. Dry compressive strength

The compressive strength of hardened pastes of M0-SH, M0-SH/LSS, M5-SH and M5-SH/LSS pastes cured in tap water (TW) then dried at 80 °C for 24 h are graphically plotted in Fig. (6). The dry compressive strength of GBFS activated by SH/LSS pastes with/without EG are higher than those of GBFS-SH mixes at all ages of curing. This is related to that, the siloxnate groups in LSS act as inorganic monomers which react with retained CH in the system or with aluminates species in the presence of Ca ions to form CSH and CASH products leading to fill some of open pores, and thereby, the compressive strength increases. The addition of EG to GBFS-SH significantly increases the dry compressive strength while it has a little effect on GBFS-SH-LSS system. This is due to the total porosity of GBFS pastes activated by SH is higher than that of GBFS pastes activated by SH/LSS. So, the EG added to the GBFS-SH system polymerized during drying process in open pores leads to decrease the porosity and consequently increase the compressive strength. This can be observed from the decrease of water absorption as a result of the addition of 5 wt, % EG to GBFS-SH system (the lower the water absorption, the lower the total of porosity of the system). Meanwhile, the total porosity in GBFSSH/LSS is very low compared to GBFS-SH system. Therefore, the addition of 5 wt%, of EG to this system has marginal effect in the development of the compressive strength. On the other hand, the dry compressive strength values of M0-SH/LSS and M5-SH/LSS gradually increases with curing time. This is due to the degree of crystallinity of CSH gel as well as CASH formed in GBFS-SH/LSS enhances during process which in turn positively affect the compressive strength values at all ages of hydration.

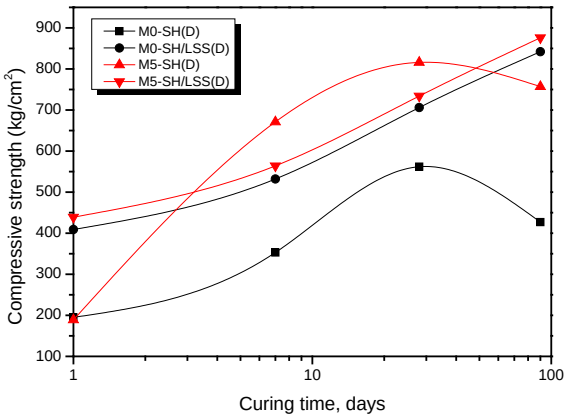

Fig. 6 Dry compressive strength of different AAS pastes with/without EG

The compressive strength values of M0-SH and M5-SH pastes increases with curing time up to 28 days then decreases up to 90 days. This reduction in compressive strength may be explained by the high increase in crystallinity degree hydration products formed in the samples. Originally, degree of crystallinity of CSH formed in GBFS-SH is higher than that formed in GBFS-SH/LSS system at room temperature. The crystallinity degree increases with the increase of temperature. The increase in crystallinity degree may cause the increase in total porosity of the system leading to decrease the compressive strength values. The addition of 5% EG to GBFS-SH system reduces the regression of compressive strength caused bydrying at 90 days. This is due to that the EG polymerized in open pores leading decreases porosity and, therefore, the compressive strength enhances.

3.5. Linear drying shrinkage

The linear drying shrinkage of GBFS pastes activated by SH or SH/LSS with 0 or 5wt, % of EG is shown in Fig. (7). It is shown that, the linear dry shrinkage of GBFS activated by SH/LSS is higher than that activated by SH. This is attributed to the amount of water absorbs by sodium silicate, which evaporates during drying of sample causing a significant effect on the linear shrinkage. The addition of EG to activated GBFS by SH or SH/LSS decreases the shrinkage by ≈ 34 and 32 %, respectively after 90 days in 50 % RH. This is attributed to that, EG helps in water retention [37].

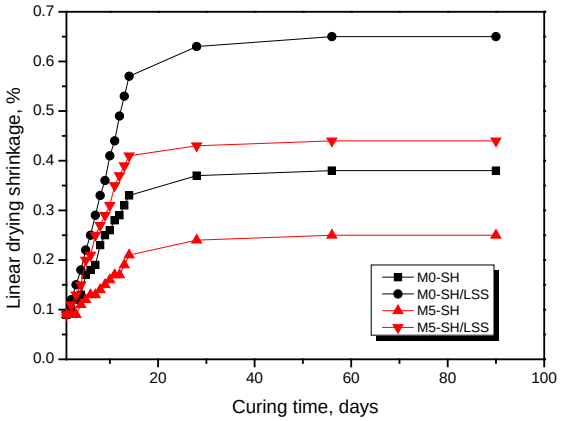

Fig. 7 Linear drying shrinkage of AAS pastes with/without EG

3.6. FTIR spectroscopy

Figure (8) illustrates the FTIR- spectra of GBFS pastes activated with mixture of 3% SH and 3% LSS (M0-SH/LSS) at one, 28 and 90 days. Obviously, the intensity of absorption band characteristics for asymmetric stretching vibration of Si–O–T (where T is Si or Al) at 967-976 cm^{-1} increases with curing time. Also, FWHM of this band decreases with curing time. These facts should be related to that the amount and degree of CSH crystallinity increase with time. The absorption band related to bending vibration of H: OH at 1644 cm^{-1} and stretching vibration of OH group at 3447 cm^{-1} after 1 day of curing are more intense than that of sample cured at 28 and 90 days. This is due to that the LSS absorb a lot amount of water at early age of curing which consumed with curing time during activation of GBFS.

Figure (9) presents the FTIR- spectra of GBFS pastes activated with mixture of 3% SH and 3% LSS containing 5 wt,% EG (M5-SH/LSS) at 1, 28 and 90 days of curing. FWHM of asymmetric stretching vibration of Si stretching vibration of Si–O–T at 965-966 cm^{-1} decreases with curing time, suggesting the increase in the degree of crystallinity which caused by the ordering of thestructure of CSH. Also, the intensity of this band increases with time. This is attributed to that the amount of CSH increases with time. These facts are in agreement with the compressive strength results. The intensity of the absorption bands related to bending vibration of HOH at 1606 cm^{-1} and stretching vibration of OH groups at 3435 cm^{-1} after 1 day are higher than those of cured after 28 and 90 days of curing. This is attributed to that, EG is polymerized to form PEG with low content of water. In addition, the intensity of these bands after 90 days is higher than those of 28 days. This is proves that the amount of CSH increases with curing time up to 90 days.

Figure (10) shows the FTIR- spectra of GBFS pastes obtained for mixes M0-SH/LSS and M5-SH/LSS after 90 days. It is clear that, the FWHM of absorption band related to asymmetric stretching vibration of Si–O–T at 969 cm^{-1} for M0-SH/LSS is lower than that of obtained for M5-SH/LSS, suggesting the formation of hydration products with low degree of crystallinity in case of M5-SH/LSS as compared with M0-SH/LSS. Conversely the intensity of absorption bands correspond to bending vibration of HOH at 1649 cm^{-1} and stretching vibration ofOH groups at 3446 cm^{-1} of M5-SH/LSS are higher than those of obtained for M0-SH/LSS. This fact may be explained by the formation of CSH in conjunction with PEG along matrix of alkali activated GBFS pastes containing 5% EG.

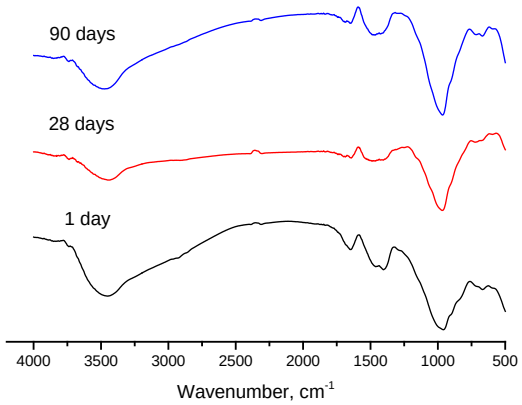

Fig. 8 FTIR-spectra of M0-SH/LSS pastes cured at 1, 28 and 90 days

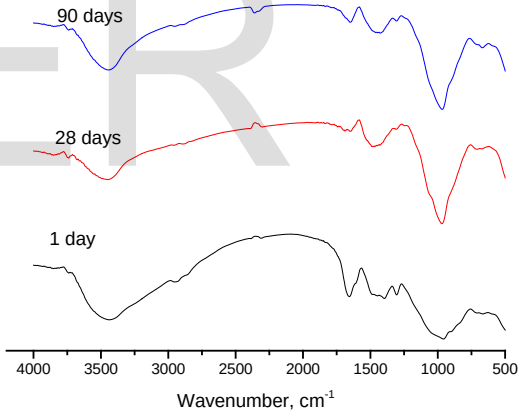

Fig. 9 FTIR-spectra of M5-SH/LSS pastes cured at 1, 28 and 90 days

Figure (11) illustrates the FTIR- spectra of GBFS pastes obtained for mixes M0-SH, M0-SH/LSS, M5-SH and M5-SH/LSS after 90 days of curing. It is shown from the comparison between the two mixes of GBFS-SH system with or without EG and GBFS-SH/LSS system the FWHM of absorption band related to asymmetric stretching vibration of Si–O–T at 965 and 967 cm^{-1} obtained for M0-SH and M5-SH mixes is lower than that obtained for M0-SH/LSS and M5-SH/LSS mixes. This demonstrated that the higher degree of CSH formed in GBFS-SH system than that of formed in GBFS-SH/LSS system.

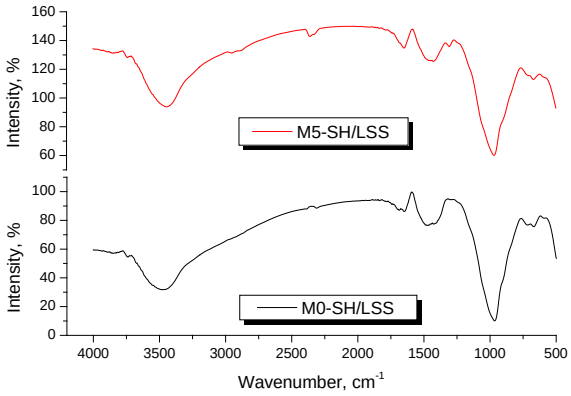

Fig. 10 FTIR-spectra of M0-SH/LSS and M5-SH/LSS cured at 90 days

Besides, the intensity of absorption bands related to bending vibration of HOH at 1700 and 1649 cm^{-1} and stretching vibration of OH groups at 3515 and 3446 cm^{-1} obtained for M0-SH/LSS and M5-SH/LSS mixes are lower than that of obtained from M0-SH and M5-SH mixes. This is attributed to the addition of LSS increase the amount of silicate species in the medium which reacts with the retained CH in the system forming CSH. Moreover these silicate species increase the degree of polymerization of hydration products formed as result of activation of GBFS (the higher the degree of polymerization, the lower the content of product). The amount of CC formed in case of M0-SH/LSS and M5-SH/LSS mixes was lower than that of formed in case of M0-SH and M5-SH mixes. This may be explained by the presence of silicate species in M0-SH/LSS and M5-SH/LSS mixes which react with remaining CH in the system to form CSH, thus, the carbonation degree decreases. This can be observed from the lower intensity band at 1514 and 1403 cm^{-1}. The intensity of this band decrease with the addition of EG suggesting that the EG polymerized in open pores in the matrix leading to the total porosity of the system, therefore, the probability of carbonation decreases.

3.7. Thermogravemetric analysis (TG/DTG)

Figure (12) presents TG/DTG of M0-SH/LSS hardened pastes cured in TW at 25°C after 1, 28 and 90 days. The weight loss of activated GBFS sample increases with the increase of curing time up to 90 days of curing as shown in TG curves (Fig. 12), suggesting the continuous activation of GBFS hydration and accumulation of hydration products as seen in Fig. 13b. Unlike the findings of TG/DTG of GBFS-SH activated system, the peak of CH is not observable in GBFS-SH/LSS activated system at all ages of curing. This should be explained by the reaction between CH and silicate species of LSS forming additional CSH.

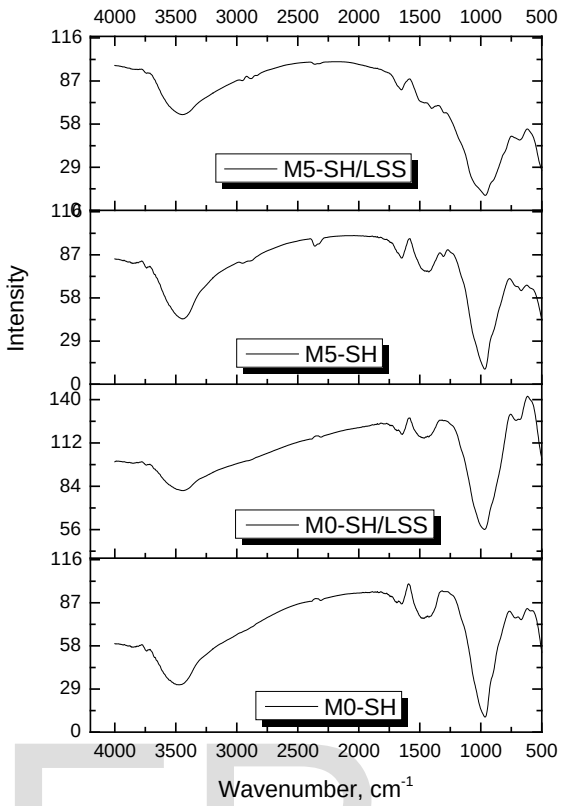

Fig. 11 FTIR-spectra of AAS pastes with/without EG after 90 days

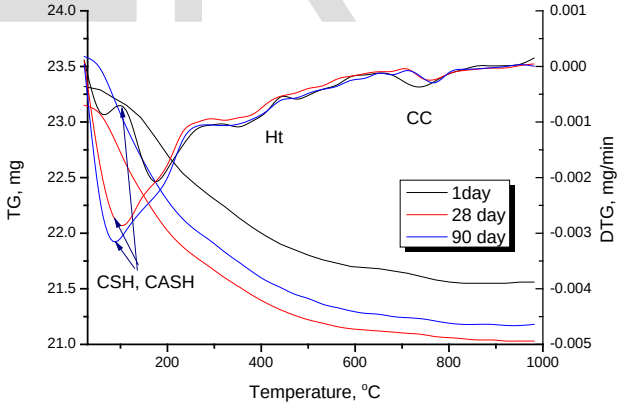

Fig. 12 TG/DTG of M0-SH/LSS pastes cured at 1, 28 and 90 days

Figure (13) shows TG/DTG of M5-SH/LSS pastes cured in TW at 25°C after 1, 28 and 90 days.Obviously, the weight loss of M5-SH mix(Fig. 13) at 1 day is greater than that at 28 and 90 days. This fact must be explained by the presence of unpolymerized EG in activated GBFS matrix that can be observed from the increase in peak intensity around 50-200°Cin DTG curves (Fig. 13). On the other hand, the weight loss of this sample cured at 90 days is greater than that of at 28 days of hydration, indicating that the amount of hydration products increases with curing time. The intensity of the peak

characteristics for the dehydration of EG that observed around 490°C decreases with curing time.This means that the degree of polymerization of EG increases with curing time. This finding is in a good agreement with the chemically combined water contents.

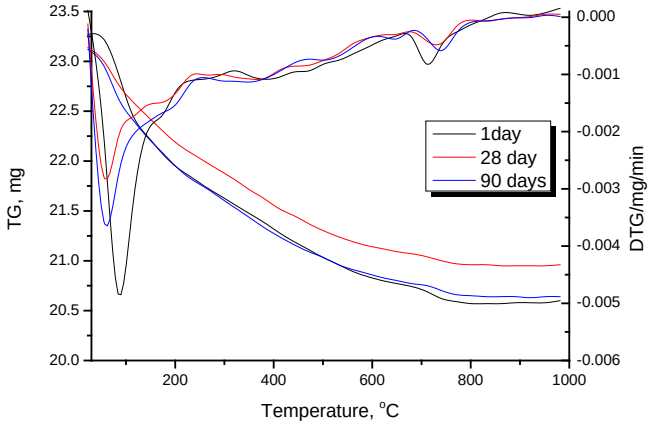

Fig. 13 TG/DTG of M5-SH/LSS pastes cured at 1, 28 and 90 days

3.8. Scanning electron microscopy (SEM)

Figure (14) represents the SEM micrographs of M0-SH/LSS cured in TW at one, 28 and 90 days. It is obvious that, there is a great gel formed along activated GBFS matrix which referred to the formation of CSH, CASH and/or silica gel (silica gel formed as a result of the presence of LSS). This gel is polymerized with curing time to give a dense microstructure, homogeneous and very compact. This confirms the compressive strength results.

Fig. (15) shows the SEM micrographs of M5-SH/LSS hardened pastes at 1, 28 and 90 days. It is clear that, the PEG is not observed at one day, suggesting that EG acts as dehydration agent for sodium silicate forming high amount of silica gel which cover the observation of PEG along the matrix [36]. The microstructure of activated GBFS seems to be unordered, unhomogeneous having a lot amount of unreacted slag grains at one day. This confirms the FTIR and compressive strength results. After 28 days of curing, the microstructure becomes a dense and ordered, due to the continuous activation and formation of hydration products as well as polymerization of EG. At 90 days the microstructure seems to be more crystalline as compared with one and 28 days. Small cracks can be observed along the paste as a result of drying shrinkage. A crystalline PEG with rode shape was observed along the paste at 90 days.

M0-SH/LSS one day

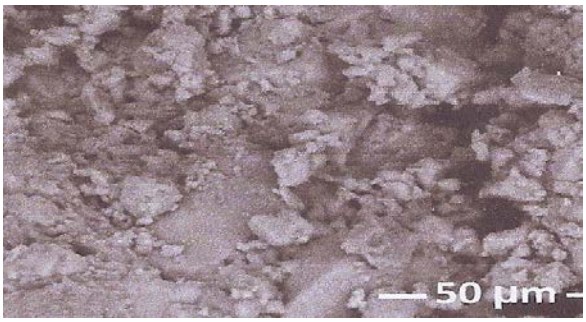

M0-SH/LSS 28 days

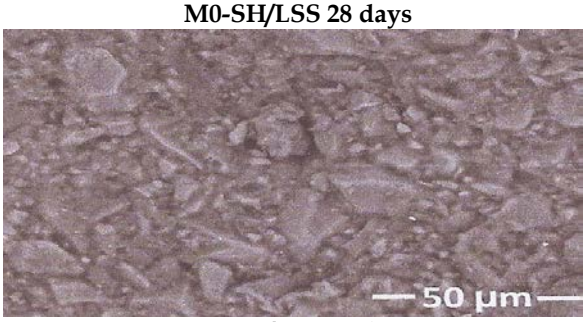

M0-SH/LSS 90 days

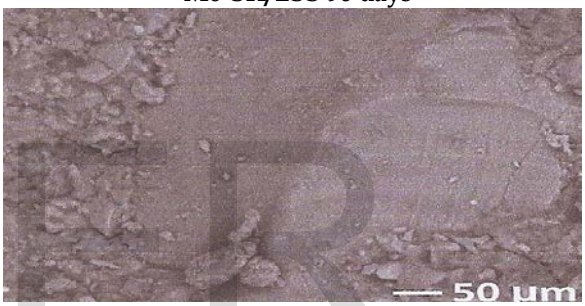

Fig. 14 SEM micrographs of M0-SH/LSS pastes cured at 1, 28 and 90 days

4. Resistivity of GBFS-SH or GBFS-SH/LSS with/without EG against $MgSO_4$ solution

4.1. Compressive strength

Figure (16) represented the compressive strength of GBFS activated by SH or SH/LSS with/without 5 wt, % EG compared with SRC pastes immersed in 5 % $MgSO_4$ solution up to 9 months. It is obvious that, all active GBFS hardened pastes with/without EG have higher resistivity against 5 % $MgSO_4$ solution. This is due to the absence of CH in activated GBFS pastes. A significant increase in the compressive strength was observed in case of pastes with EG. This is attributed to the rate of polymerization of sodium ethylene glycoxide produced during reaction between EG and SH, increases with immersing time. In contrast, there is a regular increase in the compressive strength of SRC up to 6 months followed by a significant regression up to 9 months. This is attributed to that, at first 6 months of immersion, $MgSO_4$ accelerates SRC paste hydration, leading to forming desired amount of ettringite along the matrix beside CSH, which in turn decreases the porosity and therefore increases the compressive strength. After 9 months, the amount of ettringite increases forming cracks which affects negatively the compressive strength. Moreover, Mg^{2+} reacts with CSH

forming magnesium silicate hydrate ($4MgO.SiO_2.8.5H_2O$) which has no binding properties of compressive strength, and in the presence of SO_4^{2-} gypsum is formed. It can be concluded that, AAS is more durable in $MgSO_4$ solution than SRC.

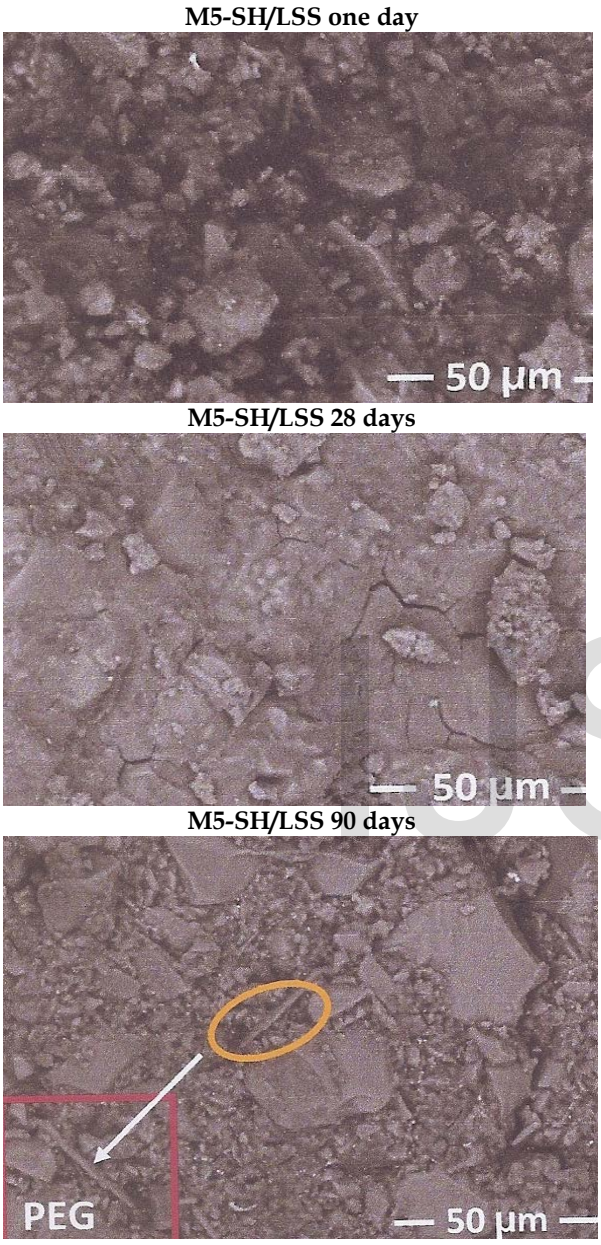

Fig. 15 SEM micrographs of AAS with 5 % EG cured up to 3, 28 and 90 days at one, 28 and 90 days

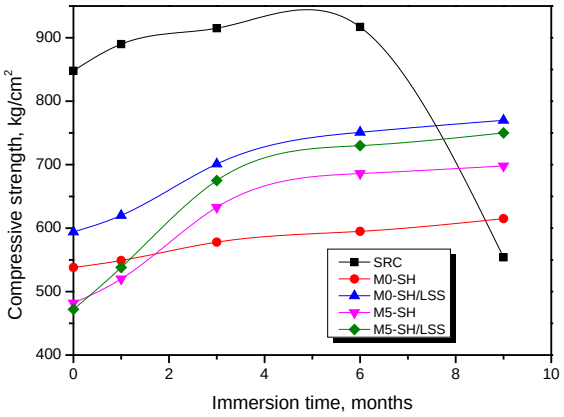

Fig. 16 Compressive strength of SRC and AAS pastes immersed in $MgSO_4$ solution up to 9 months

4.2. FTIR-spectroscopy

Fig. (17,18) illustrate the FTIR-spectra of hydrated M0-SH, M0-SH/LSS after 28 days (Zero time) and after 9 months of immersion in 5% $MgSO_4$ solution. It is shown that, there is no new band observed as a result of the immersion of all mixes in $MgSO_4$ solution. Meanwhile, a significant increase of the intensity of the main absorption band at 968-956 cm^{-1} correspond to asymmetric stretching vibration of Si-O-T was observed. Also, a reduction in FWHM as well as shifts to lower wavenumber were noted in this band for all pastes after 9 months of immersion, In addition, the intensity of absorption band related to CSH at 3450-3468 cm^{-1} of all pastes at 9 months of immersion is higher than that at zero time. These are due to that, $MgSO_4$ accelerates the activation of GBFS leading to formation more hydration products as well as increase the crystallinity which caused by ordering of calcium aluminosilicate network. This confirms the strength development during immersion in magnesium sulfate.

Fig. (19) shows FTIR spectra of SRC as well as GBFS activated by SH or SH/LSS with/without EG cured at 9 months in 5 % $MgSO_4$ solution. It is clear that, the presence of an absorption band at 1115 cm^{-1} related to SO_4^{2-} stretching vibration was shown in case of SRC paste, indicating the formation of ettringite in cement paste. This band is not observed in any activated GBFS pastes with or without EG, suggesting their higher resistivity against $MgSO_4$ solution.

Fig. (20) shows the SEM microstructures for SRC and GBFS activated by (SH or SH/LSS) pastes with/without 5 wt, % EG immersed in $MgSO_4$ solution up to 9 months. It is clear that, the SEM microstructure of GBFS-SH/LSS with/without EG indicated more compact with ordered and denser microstructure than those of GBFS-SH system. This may be explained by the presence of $[SiO_4]^{2-}$ group in LSS, which increases the degree of polymerization forming hydration product, with long chain series. Furthermore, $[SiO_4]^{2-}$ reacts with remaining Ca^{2+} and Mg^{2+} forming more CSH and MSH (magnesium silicate hydrate). This confirmed the compressive

strength results. A great amount of ettringite with crystalline needle bundle was observed in case of SRC paste, due to the migration of sulfate ions into the activated slag matrix and react with portlandite (CH) to generate gypsum with the presence of sufficient sulfate ions. AAS pastes don't have CH and monosulphoaluminate. So, when the mixes are exposed to sulfate solution, there is no formation of gypsum and ettringite formed in its matrix. This means that AAS with or without EG can't be corroded by sulfate attack.

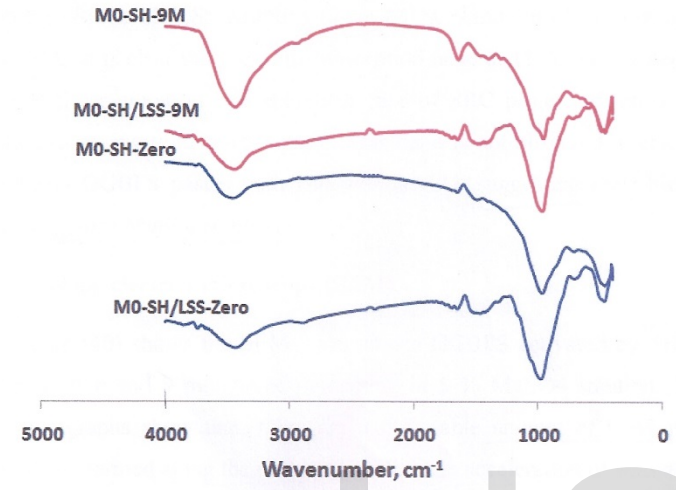

Fig. 17 FTIR-spectra of AAS by SH or SH/LSS at zero and 9 months immersed in 5% $MgSO_4$ solution.

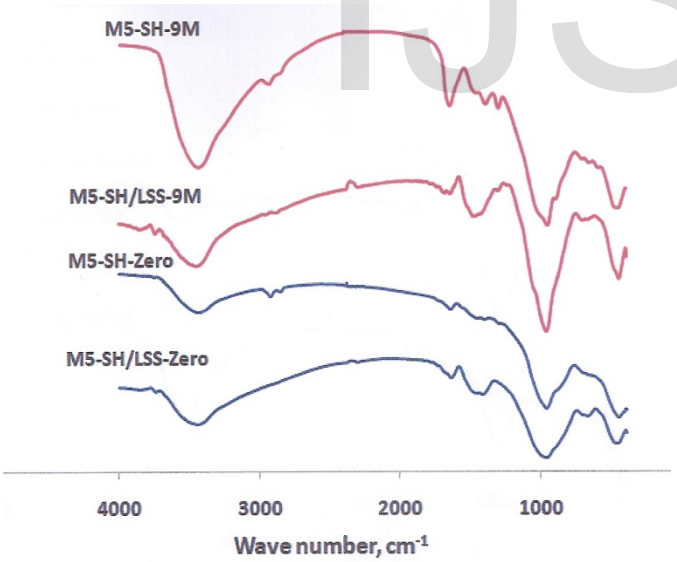

Fig. 18 FTIR-spectra of AAS by SH or SH/LSS with/without EG at zero and 9 months immersed in 5% $MgSO_4$ solution.

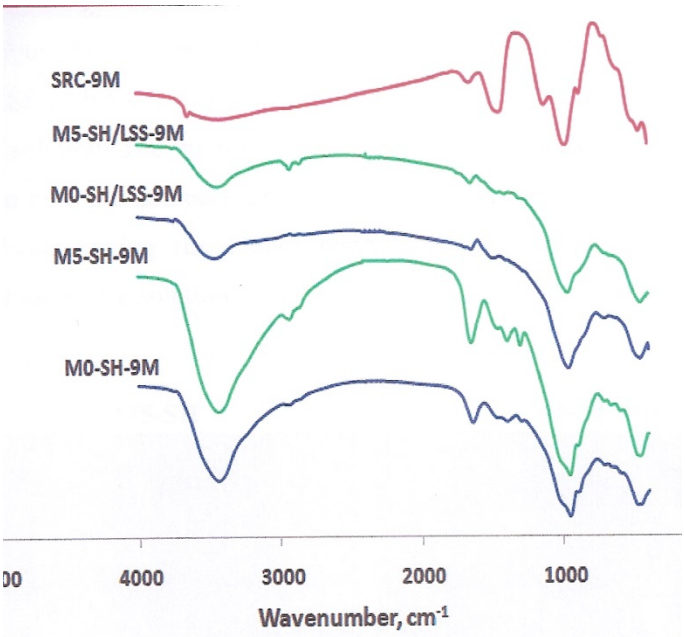

Fig. 19 FTIR-spectra of SRC as well aa AAS by SH or SH/LSS with/without EG immersed in $MgSO_4$ solution up to 9 months

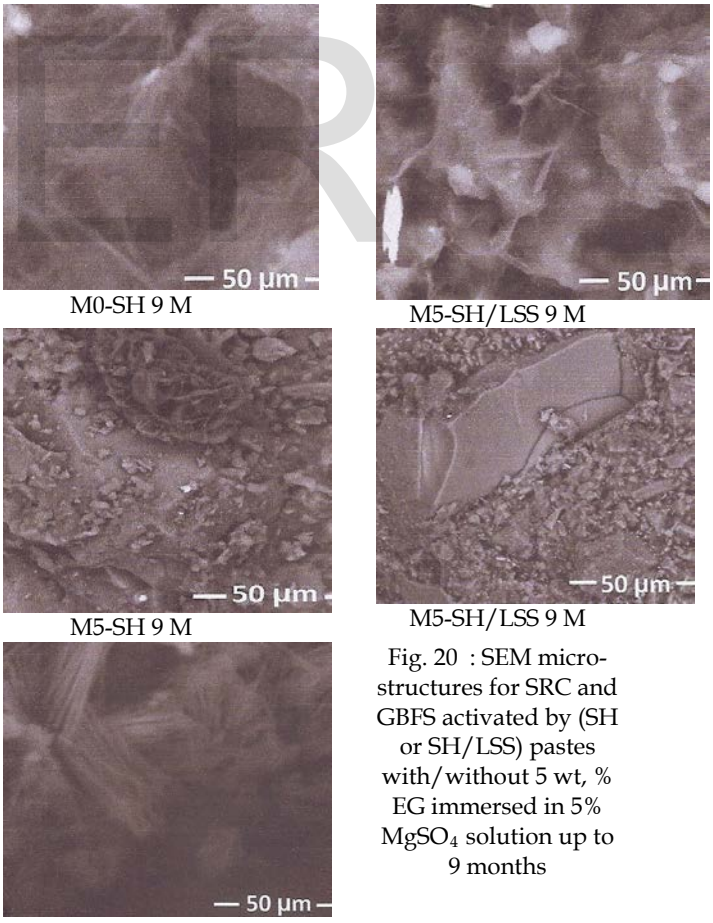

M0-SH 9 M
M5-SH/LSS 9 M
M5-SH 9 M
M5-SH/LSS 9 M

Fig. 20 : SEM micro-structures for SRC and GBFS activated by (SH or SH/LSS) pastes with/without 5 wt, % EG immersed in 5% $MgSO_4$ solution up to 9 months

CONCLUSION

From the above findings it can concluded that:

1. The initial and final setting times of M0-SH/LSS are longer than M0-SH.
2. The addition of EG to GBFS activated by SH or SH/LSS elongates the setting times.
3. The chemically combined water content of M0-SH/LSS or M5-SH/LSS is lower than that of M0-SH at all ages of hydration. In M5-SH and M5-SH/LSS pastes, the Wn, % decreases with curing time up to 28 days, then increases up to 90 days.
4. The results of combined water are in a good harmony with TG/DTG and FTIR.
5. The addition of EG to GBFS-SH system has a positive effect on the compressive strength values, while its effect on GBFS-SH/LSS has a negative effect.
6. EG added reduces the drying shrinkage of GBFS activated by SH or SH/LSS by ≈ 34 and 32 % respectively.
7. ASS paste is more durable in $MgSO_4$ solution than SRC paste.

REFERENCES

[1] A. Fernandez-Jiménez, J.G. Palomo, F. Puertas, "Alkali-activated slag mortars: mechanical strength behavior", Cem. Concr.Res., 29, pp.1313–1321, 1999.

[2] S.D. Wang, KL. Scrivener, P.L.Pratt, "Factors affecting the strength of alkaliactivated slag", Cem.Concr.Res., vol. 24(6), pp. 1033–1043, 1994.

[3] M. Criado, A. Fernandez-Jiménez, A.G. De la Torre, M.A.G. Aranda, A. Palomo, "An XRD study of the effect of the SiO_2/Na_2O ratio on the alkali activation of fly ash", Cem. Concr.Res., vol. 37, pp. 671–679, 2007.

[4] H. El-Didamony, A.A. Amer, H. AbdEla-ziz, Properties and durability of alkali-activated slag immersed in sea water, Cera. Intern., vol. 38(5), pp 3773-3780, 2012.

[5] T. Bakharev, J.G. Sanjayan, Y.B. Cheng, "Resistance of alkali-activated slag concrete to acid attack", Cem. Concr. Res.,vol. 33, pp.1607–1611, 2003.

[6] F. Puertas, R.D. Gutierrez, A. Fernández-Jiménez, S. Delvasto, J. Maldonado,. "Alkaline cement mortars. Chemical resistance to sulfate and seawater attack." Materiales de Construccion, Vol. 52, No. 267, pp. 55-71, 2002.

[7] D.L.Y. Kong, J.G.Sanjayan, "Damage behavior of geopolymer composites exposed to elevated temperatures", Cem. Concr.Compos., vol. 30, pp. 986–991, 2008.

[8] Y.Z. Hai, VenkateshKodur, L.Q. Shu, C. Liang, W.Bo "Development of metakaolinfly ash based geopolymers for fire resistance applications", Constr. Build.Mater., vol. 55, pp. 38–45, 2014.

[9] M. Weil, K. Dombrowski, A. Buchawald, "Life-cycle analysis of geopolymers. Geopolymers, structure, processing, properties and applications", Abington Hall: Woodhead Publishing Limited, pp. 194–210, 2009.

[10] C. Bilim, O. Karahan, C.D. Atis, S. Ilkentapar, Effects of chemical admixtures and curing conditions on some properties of alkali-activated cementless slag mixtures, KSCE J. Civil. Engin. Vol. 19(3), pp. 733-741, 2015

[11] S. Song, D. Sohn, H.M. Jennings, T.O. Mason, Hydration of alkali-activated ground granulated blast furnace slag., J. Mater. Sci., vol. 35, pp 249-257, 2000.

[12] C.K. Yip, G.C. Lukey, J.S.J. van Deventer, The coexistence of geopolymeric gel and calcium silicate hydrate at the early stage of alkaline activation, CemConcr Res., vol. 35, pp. 1688-1697, 2005.

[13] A.R. Brough, A.Atkinson, "Sodium silicate-based alkali-activated slag mortars: Part I. Strength, hydration and microstructure", Cem. Concr.Res., 32, pp. 865–79, 2002.

[14] S. Chithiraputhiran, N. Neithalath, Isothermalreaction kinetics and alkali activation of slag, fly ash, and their blends.Construction and Building Materials, 45, 233–242, 2013.

[15] E. Altan, S.T. Erdog˘an, Alkali activation of a slag at ambient and elevated temperatures. Cement & Concrete Composites, vol. 34, pp.131-139, 2012.

[16] J.J. Chang, A study on the setting characteristics of sodium silicate-activated slag pastes. Cement and Concrete Research, vol. 33, 1005-1011, 2003.

[17]] A. De Roma, H.J. Yang, S. Milione, C. Capacchione, G. Roviello, A.Grassi, "Atom transfer radical polymerization of methylmethacrylate mediated by a naphtyl-nickel(II) phosphane complex", Inorg. Chem. Commun., 14, pp. 542–544, 2011.

[18] I. D"Auria, M. Lamberti, M.Mazzeo, S. Milione, G.Roviello, C. Pellecchia, "Coordination chemistry and reactivity of zinc complexes supported by a phosphido pincer ligand", Chem. Eur. J., 18, pp. 2349–2360, 2012.

[19] G..N. Roviello, G. Roviello, D. Musumeci, E.M., C. BucciPedone, "Dakin-west reaction on 1-thyminyl acetic acid for the synthesis of 1,3-bis(1-thyminyl)-2-propanone, a heteroaromatic compound with nucleopeptide-binding properties", Amino. Acids., 43, pp. 1615–1623, 2012.

[20] A. Carella, F. Borbone, A. Roviello, G. Roviello, A. Tuzi, A. Kravinsky, R.Shikler, G. Cantele, D. Ninno, "Benzodifuroxazinones, a new class of heteroacene molecules for possible applications in organic electronics: Synthesis, electronic properties and crystal structure", Dyes Pigments., 95, pp. 116–125, 2012.

[21] G. Li, M. Lamberti, G. Roviello, C. Pellecchia, "New titanium and hafnium complexes bearing [-NNN-] pyrrolyl-pyridylamido ligands as olefin polymerization catalysts", Organometallics., 31, pp. 6772–6778, 2012.

[22] A. Roviello, A. Buono, A. Carella, G. Roviello, A. Cassinese, M. Barra, M. Biasucci, "Regioregularpoly[3-(4-alkoxyphenyl) thiophene]s", J. Polym. Sci. Pol. Chem., 45, pp. 1758–1770, 2007.

[23] Y.J. Zhang, S. Li, D.L. Xu, B.Q. Wang, G.M. Xu, D.F. Yang, N. Wang, H.C. Liu, Y.C. Wang, "A novel method for preparation of organic resins reinforced geopolymer composites", J. Mater. Sci., 45, pp. 1189–1192, 2010.

[24] Z. Zhang, X. Yao, H. Zhu, S. Hua, Y. Chen, "Preparation and mechanical properties of polypropylene fiber reinforced calcined kaolin-fly ash based geopolymer", J. Cent. South. Univ. Technol., 16, pp. 49–52, 2009.

[25] Y. Zhang, W. Sun, Z. Li, "Impact behavior and microstructural characteristics of PVA fiber reinforced fly ash-geopolymer boards prepared by extrusion technique", J. Mater.Sci., 41, pp. 2787–2794, 2006.

[26] Y. Zhang, W. Sun, Z. Li, X. Zhou, "Impact properties of geopolymer based extrudates incorporated with fly ash and PVA short fiber", Constr. Build. Mater., 22, pp. 370–383, 2008.
[27] S. Zhang, K. Gong, J. Lu, "Novel modification method for inorganic geopolymer by using water soluble organic polymers", Mater.Lett., 58, pp. 1292–1296, 2004.
[28] C. Ferone, G. Roviello, F. Colangelo, R. Cioffi, O. Tarallo, "Novel hybrid organic-geopolymer materials" Appl. Clay Sci., 73, pp. 42–50, 2013.
[29] H. El-Didamony, A. Amer, M. Arif, Impact of ethylene glycol addition on the physico-chemical and mechanical properties of alkal-activated GGBFS pastes, Inter. J Sci. & Res. (IJSR), vol. 4(5), pp 1596-1605, 2015.
[30] M. Komljenović, Z. Bašcarević, N. Marjanović, V. Nikolic, External sulfate attack on alkali-activated slag, Constr. Build. Mater.,vol 49, pp. 31-39, 2013.
[31] T. Bakhareva, J.G. Sanjayana, Y.B. Chengb, Resistance of alkali-activated slag concrete to acid attack, Cem. Concr.Res., vol 33, pp.1607-1611, 2003.
[32] ASTM C 191-13, "Standard Test Methods for Time of Setting of Hydraulic Cement by Vicat Needle".
[33] I. Soroka, Portland cement paste and concrete, London: The Macillan Press Ltd., 1986.
[34] ASTM C109M, "Standard test method for compressive strength of hydraulic cement mortars", 2012.
[35] ASTM C490, "Standard practice for use of apparatus for the determination of length change of hardened cement paste, mortar, and concrete", 2007.
[36] A. Baliński, Nanostructure of the soluble sodium silicate in the aspect of basic mechanical characteristic of the moulding sand, Econtechmod. An Inter. Quarterly J, vol. 1(1), p. 03-08, 2012.
[37] C. Kuenzel, L.J. Vandeperre, S. Donatello, A.R. Boccaccini, C. Cheeseman, "Ambient temperature drying shrinkage and cracking in metakaolin-based geopolymers", J. Am. Ceram. Soc., 95, pp.3270–3277, 2012.